

# Variations in alumina-based material composition and heating temperature of refractory bricks in mullite formation

David Candra Birawidha<sup>1\*</sup>, Muhammad Amin<sup>1</sup>, Agus Miswanto<sup>2</sup>, Fery Hendi Jaya<sup>3</sup>, Sari Utama Dewi<sup>3</sup>, Mentari Kirana Nariswari<sup>4</sup>, Devi Mariska Putri<sup>4</sup>

<sup>1</sup> Research Center for Mining Technology, National Research and Innovation Agency (BRIN), Lampung, Indonesia

<sup>2</sup> Geological Resource Research Center, National Research and Innovation Agency (BRIN), Bandung, Indonesia

<sup>3</sup> Sang Bumi Ruwa Jurai University, Lampung, Indonesia

<sup>4</sup> Universitas Lampung, Lampung, Indonesia

\*Corresponding author: e-mail [davi004@brin.go.id](mailto:davi004@brin.go.id)

## Abstract

**Purpose.** This study investigates the effects of varying alumina content and firing temperatures on the formation of mullite in refractory bricks composed of kaolin, alumina, and recycled chamotte. The goal is to develop high-performance, cost-effective refractories using local and recycled materials.

**Methods.** Three formulations with different alumina proportions were prepared, pressed, and sintered at 1200 or 1300°C. Characterization was performed using XRF (chemical composition), XRD (phase analysis), FE-SEM/EDX (microstructure), and STA (thermal behavior). Mechanical properties were assessed using a UTM, and chemical resistance was evaluated by exposure to H<sub>2</sub>SO<sub>4</sub> and NaOH solutions.

**Findings.** Results show that higher alumina content and firing at 1300°C promote mullite formation, thereby improving mechanical strength, density, and resistance to thermal shock and chemical corrosion. The refractory with 35% alumina, fired at 1300°C, achieved the highest cold crushing strength (26.5 N/mm<sup>2</sup>) and bulk density (2.13 g/cm<sup>3</sup>), indicating optimal performance.

**Originality.** The novelty of this work lies in the strategic use of recycled chamotte, not merely as a filler, but as a functional mullite precursor that synergizes with local kaolin to enhance sintering. This approach is concretely validated by the optimal performance of the 35% alumina composition fired at 1300°C, which achieved the highest mechanical strength and density, demonstrating a cost-effective and high-performance refractory solution from sustainable sources.

**Practical implications.** The findings provide practical solutions for manufacturing high-quality refractories from sustainable, locally sourced materials, thereby reducing dependence on pure alumina and promoting environmental sustainability through recycling.

**Keywords:** refractory brick, mullite, testing, analysis, alumina

## 1. Introduction

Refractory bricks constitute essential materials in sustaining high-temperature industrial operations in Indonesia, particularly in the metallurgy, cement, and power generation sectors. These ceramics are engineered to endure mechanical stress, chemical attack, corrosion, and severe thermal gradients, making them highly suitable for applications such as furnace linings, thermal insulation, and critical components within combustion and smelting systems [1]. Based on [2], refractory materials are defined as non-metallic substances that possess the requisite physical and chemical characteristics to withstand environments exceeding 1000°F (538°C). Refractories are typically multi-phase ceramics specifically designed to perform reliably under extreme service conditions and elevated temperatures [3]. Their functionality necessitates resistance not only to exhaust gas corrosion and slag infiltration but also to cyclic thermal shocks and thermomechanical loading [4], [5].

Despite their exceptional durability, refractory bricks experience progressive degradation due to constant exposure to abrasive forces and chemical reactions, particularly during repeated thermal cycles. This wear leads to periodic replacement requirements, contributing substantially to industrial waste generation. Improper disposal of such waste poses environmental hazards, thereby necessitating the adoption of sustainable waste management strategies. The recycling of spent refractory materials presents a viable approach aligned with the principles of the circular economy and environmental stewardship within the refractory industry [6], [7].

The Indonesian Ministry of Industry (2019) reported that domestic demand for refractory products ranges between 150-200 thousand metric tons annually. However, national production capacity remains limited to approximately 50 thousand tons per year. This substantial supply gap is primarily driven by sustained demand from foundries and other thermal process industries that require routine refracto-

Received: 24 June 2025. Accepted: 16 December 2025. Available online: 30 December 2025

© 2025, D.C. Birawidha et al.

Mining of Mineral Deposits. ISSN 2415-3443 (Online) | ISSN 2415-3435 (Print)

This is an Open Access article distributed under the terms of the Creative Commons Attribution License (<http://creativecommons.org/licenses/by/4.0/>), which permits unrestricted reuse, distribution, and reproduction in any medium, provided the original work is properly cited.

ry maintenance. Consequently, the development of innovative, cost-efficient, and locally sourced refractory solutions is imperative to mitigate the supply-demand disparity.

The physicochemical properties of refractory bricks are predominantly determined by their raw material composition. Among these, alumina ( $\text{Al}_2\text{O}_3$ ) is widely utilized due to its superior thermal stability and its facilitation of mullite ( $3\text{Al}_2\text{O}_3 \cdot 2\text{SiO}_2$ ) phase formation. High-alumina refractories have demonstrated effective performance in erosive and high-temperature environments such as combustion chambers [8]. Nevertheless, the reliance on pure alumina often incurs substantial production costs, rendering conventional refractory production less economically sustainable. In response, research has increasingly focused on incorporating recycled refractory waste and abundant local raw materials, such as kaolin, to reduce cost while maintaining functional integrity. Kaolin, rich in silica ( $\text{SiO}_2$ ), exhibits insulating and thermal-resistant properties and functions as both a binder and filler during sintering. It facilitates particle cohesion, reduces porosity, and preserves mechanical strength [9]. The silica content in kaolin reacts with alumina to promote the in-situ formation of mullite phases, which are known for their low thermal conductivity, high temperature resistance, and structural stability [8]. Therefore, a composite formulation comprising kaolin and alumina presents a promising low-cost refractory alternative with high thermal performance characteristics.

Empirical evidence from various studies substantiates this methodology, which was conducted to investigate the effect of quartz sand composition, including kaolin and fly ash, on the properties of refractory bricks at a heating temperature of  $1275^\circ\text{C}$  [10]. Based on the study's results, it is evident that adding quartz sand composition increases density and thermal conductivity values. The maximum compressive strength is achieved at a 10% quartz sand addition, reaching 30.51 MPa.

El Haddar et al. researched the production of high-mechanical-performance refractories from recycled halloysite and alumina [11]. For this purpose, six mixtures (M1-M6) were tested using marl, diatomite, and silica sand aggregates to enhance halloysite performance and develop high-temperature ceramic up to  $1300^\circ\text{C}$  (silico-aluminous refractory "S-Al-R"). Among all the mixtures tested, mixture M6 demonstrates good technical quality, with porosity ( $P$ ) = 21.75%, density ( $d$ ) =  $1.94 \text{ g/cm}^3$ , thermal shrinkage ( $R$ ) = 2.7%, and flexural strength ( $R_f$ ) = 29.05 MPa. In addition to the mixture (M6) of 25% of their cycled alumina "Rec-Al", obtained from silico-aluminous refractory bricks waste, has substantially strengthened the mechanical performance of the silico-aluminous refractory ( $R_f$  = 45.08 MPa).

Amin et al. conducted a study on the characterization of refractory bricks using local raw materials in Lampung Province, Indonesia. The raw materials, including quartz sand, kaolin, bentonite, feldspar, and ball clay, were mixed and then divided into seven types of compositions [12]. The results of composition one bricks are similar to those of SK-34 type refractory bricks, with  $\text{SiO}_2$  at 54.21%,  $\text{Al}_2\text{O}_3$  at 25.38%, and density test results of  $2.25 \text{ g/cm}^3$ , porosity of 18.98%, and compressive strength of  $325 \text{ kg/cm}^2$ . It was found that the density is inversely proportional to the porosity caused by the sintering process, because the powder particles melt into a solid phase, thereby reducing the porosity value.

Based on the description above, further study and research are necessary to develop alternative solutions to ad-

dress the refractory demand for refractory bricks. This study aims to produce refractory bricks with a main oxide content of mullite by varying the composition of alumina-based materials and by varying the heating temperatures to  $1200^\circ\text{C}$  and  $1300^\circ\text{C}$  during the formation of the mullite phase. The raw materials used in the composition variations include kaolin, alumina, and chamotte.

## 2. Methods

The raw materials used in this experiment are local kaolin lampung material, alumina, and recycled chamotte from SK-34 refractory bricks. The first stage of sample preparation is cleaning the material, which is then ground separately using a Ball Mill Type TR6-ZA-D112.M4. After completion, the chamotte material is then sieved using a 10-mesh sieve as an aggregate, while kaolin is sieved using a 100-mesh sieve as a filler. Furthermore, initial characterization of the raw material is carried out with XRF and XRD analysis to determine the chemical composition and dominant phase contained in the raw material using XRF PANalytical type: Minipal 4 operating at a voltage of 30 kV, XRD PANalytical type: ExpertPro operating at a voltage of 40 kV. Then, the sintering process of the kaolin material is carried out at a temperature of  $900^\circ\text{C}$  with a heating rate of  $500^\circ\text{C}/\text{hour}$ , and it is held for 60 minutes at the specified temperature. The material is then cooled in the furnace until it reaches room temperature.

All raw materials are weighed and adjusted to account for the composition variations listed in Table 1, with a total weight of 300 g. In each composition variation, bentonite is added at an equivalent of 10% of the total weight. All the ingredients are mixed with the addition of 20% water, and the refractory brick mixture is then inserted into the mold. It is subjected to a pressure of 10 tons using a hydraulic press, a floor model Krisbow type 20 t. The molded sample is dried using a microwave advanced type AOV-300 at a temperature of  $60^\circ\text{C}$  with a hold for 60 minutes. Then, the refractory brick sample is heated/burned using a muffle furnace with a heating rate of  $500^\circ\text{C}/\text{hour}$  and held for 60 minutes at the specified temperatures of 1300 and  $1200^\circ\text{C}$ .

**Table 1. Variation of refractory brick composition**

Variation	Material, % wt			Temperature, $^\circ\text{C}$
	K	A	C	
RF20/30/50A	20	30	50	1.300
RF15/35/50A	15	35	50	1.300
RF10/40/50A	10	40	50	1.300
RF20/30/50B	20	30	50	1.200
RF15/35/50B	15	35	50	1.200
RF10/40/50B	10	40	50	1.200

The refractory brick samples were analyzed using FESEM-EDX (Thermo Scientific™ Quattro SEM) to determine the morphology, topography, and elements formed on the surface of the refractory bricks. The measurement of mass changes and thermal effects of the refractory bricks was analyzed using a NETZSCH STA 449 F3 Jupiter. The crystal structure that formed was determined by X-ray diffraction using a Panalytical X-Pert 3 Powder XRD system with Cu-K $\alpha$  as the X-ray source. The operating voltage was 40 kV, and the current was 30 mA, with the test sample scanned at an angle of  $2\theta$  from 20 to  $80^\circ$ . At the same time, the chemical composition of matter is known using X-ray fluorescence (Malvern

Panalytical’s X-RF Epsilon 4 XRF Spectrometer), operating at a voltage of 50 kV and a current of 3 mA. The measurement of the strength of refractory bricks under loading was analyzed using a Universal Testing Machine (UTM HT-2402). Then, for the calculation of density, porosity, and water absorption based on Archimedes’ method. Meanwhile, for calculating the decomposition of refractory bricks due to the heating rate, the calculation reference is ASTM C113-14 [13]. The analysis of the resistance of refractory bricks to chemical properties was conducted by providing H<sub>2</sub>SO<sub>4</sub> and NaOH solutions, followed by a reheating treatment in a muffle furnace at 1150°C. The samples were then cooled to room temperature and visually analyzed to determine the resistance of the refractory bricks to chemical properties.

### 3. Results and discussion

In the initial characterization analysis of the raw materials, it is evident from Table 2 that SiO<sub>2</sub> is the dominant element in both kaolin and chamotte, with percentages of

73.27 and 44.34% wt, respectively. In the characterization analysis of the refractory brick samples, it is known that there are alkali oxides, such as CaO, and there are Fe<sub>2</sub>O<sub>3</sub> oxides that exceed the limit value, which can affect the resistance of refractory bricks. The percentage value of Fe<sub>2</sub>O<sub>3</sub> oxide does not exceed 2.5% (wt) [14]. The dominant oxides in the refractory brick variation samples are Al<sub>2</sub>O<sub>3</sub> and SiO<sub>2</sub>, which are the oxides that form the mullite phase. The solid-phase reaction of the alumina-silica oxide mixture at high temperatures can cause the formation of mullite [15].

Figure 1a presents the XRD characterization analysis of chamotte and kaolin raw materials. The chamotte raw material contains a mullite phase, which is attributed to the use of recycled SK-34 refractory bricks as the chamotte material. Meanwhile, in kaolin, silica oxide is dominant and plays a significant role in the formation of the quartz phase.

Figure 1b, c, d present the XRD results for various refractory brick samples, revealing significant differences in their phase compositions.

Table 2. XRF analysis results (% wt)

Compound	Raw material		Sample					
	K	C	RF20/30/50A	RF15/35/50A	RF10/40/50A	RF20/30/50B	RF15/35/50B	RF10/40/50B
Al <sub>2</sub> O <sub>3</sub>	16.97	36.15	50.91	53.43	58.26	48.01	53.24	58.10
SiO <sub>2</sub>	73.27	44.34	39.37	35.89	32.42	40.64	36.15	32.39
TiO <sub>2</sub>	0.48	3.65	1.64	2.11	1.85	2.19	1.89	1.75
CaO	1.84	0.87	1.14	1.04	0.96	1.41	0.96	0.91
Fe <sub>2</sub> O <sub>3</sub>	4.30	6.62	4.44	4.95	4.15	5.14	5.02	4.45

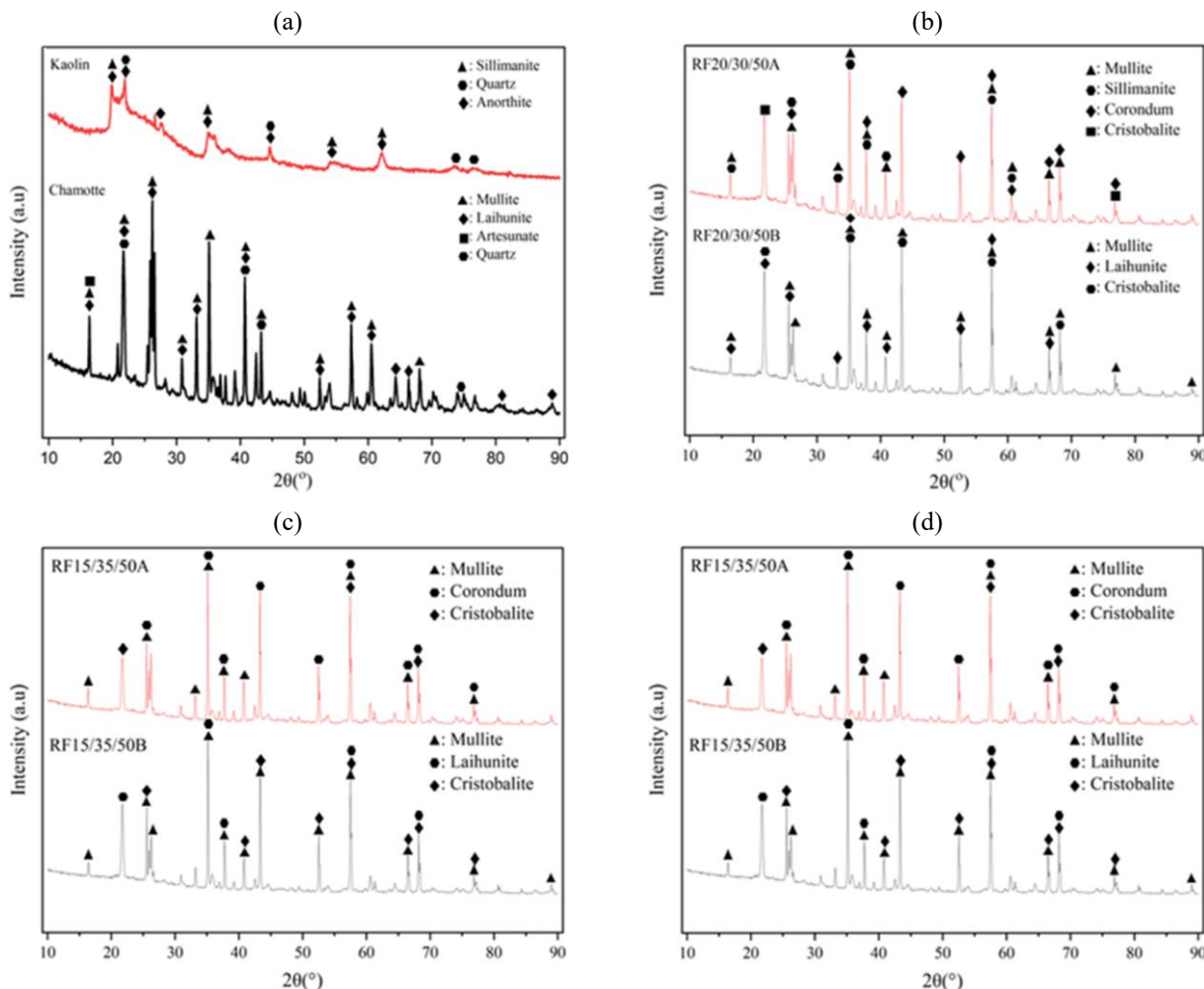


Figure 1. XRD analysis results: (a) raw material; (b) RF 20/30/50; (c) RF15/35/50; (d) RF10/40/50

Specifically, the samples treated at 1200°C show the presence of three main phases: mullite, laihunite, and cristobalite. These phases are formed under relatively lower firing temperatures and are typical of the reaction processes that occur in the silica-alumina system at temperatures just below 1300°C. In contrast, the samples fired at 1300°C (variations RF20/30/50A, RF15/35/50A and RF10/40/50A) exhibit the formation of different phases, including sillimanite, corundum, and gibbsite. These phase variations reflect the impact of temperature on the crystallization behavior and phase transitions within the refractory materials. The higher firing temperature facilitates the formation of phases such as sillimanite and corundum, which are more thermodynamically stable at elevated temperatures. In contrast, lower temperatures lead to the stabilization of phases like mullite and cristobalite [16].

The formation of mullite and cristobalite in the samples fired at 1200°C is consistent with the findings of who demonstrated that these phases tend to stabilize around 1300°C, which is considered an optimal temperature for their formation. Mullite, an alumino-silicate phase, forms as a result of the reaction between alumina oxide ( $\text{Al}_2\text{O}_3$ ) and silica ( $\text{SiO}_2$ ) at high temperatures, typically above 1200°C. The high-temperature conditions promote the interaction between these oxides, resulting in the formation of mullite crystals that significantly enhance the mechanical and thermal properties of the refractory material. The formation of cristobalite, another high-temperature polymorph of silica, is closely linked to the silica content and temperature [17]. Cristobalite is known for its high expansion coefficient, which can enhance the material's ability to withstand thermal shock. The combination of mullite and cristobalite phases in the material contributes to its ability to maintain structural integrity under rapid temperature fluctuations, making it more resistant to thermal cycling [18].

In kaolin-based materials, phase transformations occur from sillimanite ( $\text{Al}_2\text{SiO}_5$ ) to quartz ( $\text{SiO}_2$ ), and under higher temperatures, anorthite ( $\text{CaAl}_2\text{Si}_2\text{O}_8$ ) may form. These transformations result from the silica content present in kaolin and the elevated temperatures that favor the formation of more thermodynamically stable phases. The transition from sillimanite to quartz and anorthite is also influenced by the presence of fluxing agents such as calcium, which reduces the melting point of the material and facilitates the formation of stable phases at high temperatures. This transformation not only alters the crystalline structure of the material but also affects its overall physical properties, including density, strength, and porosity [19].

Chamotte, which is primarily composed of alumina and silica, undergoes significant phase transformations at higher firing temperatures. Mullite, which forms as the primary phase at moderate temperatures, transforms laihunite, artesunate, and quartz at 1300°C. These transformations occur due to the complex interactions between alumina and silica, along with the influence of other elements such as calcium, magnesium, and iron, which can act as fluxing agents. Laihunite is a calcium aluminosilicate phase that can form when the alumina-silica ratio is altered, and it contributes to the material's improved high-temperature stability. Artesunate, a less common phase, can form in the presence of specific temperature and pressure conditions, and it further enhances the material's structural properties by improving its resistance to high-temperature deformation.

These phase transformations in chamotte are essential for improving the thermal stability, mechanical strength, and structural integrity of the material. The transition from mullite to laihunite, artesunate, and quartz helps create a more stable and durable material, which is particularly important for refractories used in high-temperature applications. Mullite's role in enhancing the high-temperature stability of the material is well documented, as it contributes to the refractory's resistance to deformation and thermal shock. Cristobalite and talc, both high-temperature phases, further enhance the material's ability to resist thermal shock by increasing its capacity to absorb and dissipate thermal stresses during rapid temperature changes [20]. These phase transitions, therefore, play a critical role in improving the performance of refractory materials, making them more durable and resilient under extreme temperature conditions.

Figure 2 shows the results of the STA characterization analysis of the refractory brick variation samples. Simultaneous Thermal Analysis (STA) is a sophisticated analytical method that integrates Thermogravimetric Analysis (TGA) and Differential Scanning Calorimetry (DSC), allowing for the simultaneous measurement of changes in sample mass and heat flow as a function of temperature or time. This dual approach enables a thorough characterization of the thermal properties and reactions of materials under precisely controlled conditions [21].

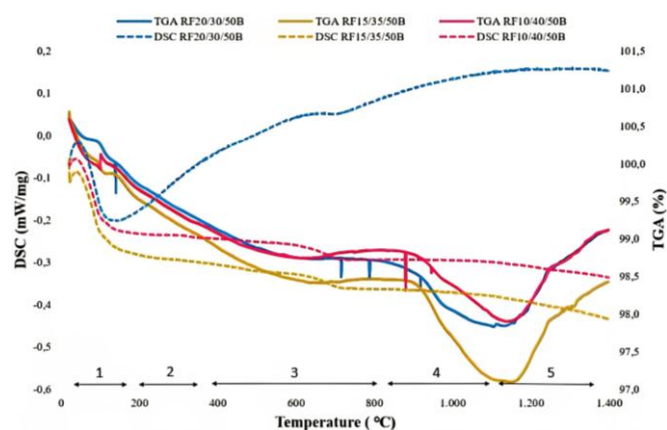


**Figure 2. Thermal behavior and phase transformation analysis: 1 – initial heating; 2 – release of carbon compounds; 3 – decomposition of heating rate; 4 – oxidation of compounds; 5 – mullite phase transformation**

According to Yue et al., initially below 600°C, the thermogravimetric analysis (TGA) indicates mass loss primarily due to the evaporation of moisture and the dehydroxylation of hydroxides present in the material matrix [22]. The corresponding endothermic peaks in the differential scanning calorimetry (DSC) curve confirm the absorption of energy during these dehydration processes. The corresponding endothermic peaks in the differential scanning calorimetry (DSC) curve confirm the absorption of energy during these dehydration processes.

Between 600 and 900°C, the mass loss slows, indicating the completion of volatile release. DSC reveals exothermic events corresponding to phase transformations such as crystallization and grain growth, which are essential for improving the refractory's mechanical properties and thermal shock resistance [23]. Between 900 and 1200°C, sintering and densification dominate, as indicated by stabilized TGA

data and subtle DSC exothermic peaks. These changes reduce porosity, enhance grain boundary bonding, and improve thermal conductivity and structural integrity [24]. The stabilization of mass and reduced thermal events near 1200°C indicate the refractory's high-temperature durability, which is critical for applications in furnaces and kilns.

These findings align with recent literature emphasizing that the performance of refractory materials depends on controlled phase changes and minimal mass loss to maintain structural and chemical stability at elevated temperatures [25].

The SEM analysis results presented in Figure 3a-f indicate that the topography of each sample variation shows the presence of pore cavities, which are typically formed due to the distribution of impurities within the material. These pores are evident across the different sample variations and can significantly affect the physical and mechanical properties of the refractory bricks. The pore cavities often result from factors that hinder the rearrangement of the ceramic matrix during the heating process, such as the presence of residual impurities. These impurities prevent the material from uniform densification, leading to the formation of voids or gaps within the brick structure.

The presence of these pore cavities is critical, as they can negatively influence the mechanical strength of the refractory material. Pore cavities reduce the overall density

of the material, and their distribution within the ceramic body is directly related to its diametric strength. The strength of refractory bricks, particularly their resistance to mechanical stress, is heavily influenced by the proportion of pores present. A higher percentage of pores typically leads to a decrease in the material's strength, making it more susceptible to failure under load or during thermal cycling.

Additionally, the pore cavities can impact the material's thermal conductivity and thermal shock resistance. As the pores increase, the material's ability to withstand rapid temperature changes or extreme heat is compromised, leading to a reduction in the brick's effectiveness in high-temperature applications. The formation of these pores is especially concerning in industrial applications, where refractory bricks are subject to harsh conditions, and any reduction in mechanical or thermal properties can lead to premature failure.

When comparing the different samples treated at varying temperatures, it is observed that the sample treated at 1300°C exhibits fewer and smaller pore cavities than the one treated at 1200°C. This is indicative of the effect that heat treatment temperature has on the densification process. Higher temperatures promote better sintering, which helps reduce the formation of pore cavities. Conversely, the sample treated at the lower temperature of 1200°C exhibits a greater number of larger voids, indicating insufficient sintering and incomplete impurity elimination.

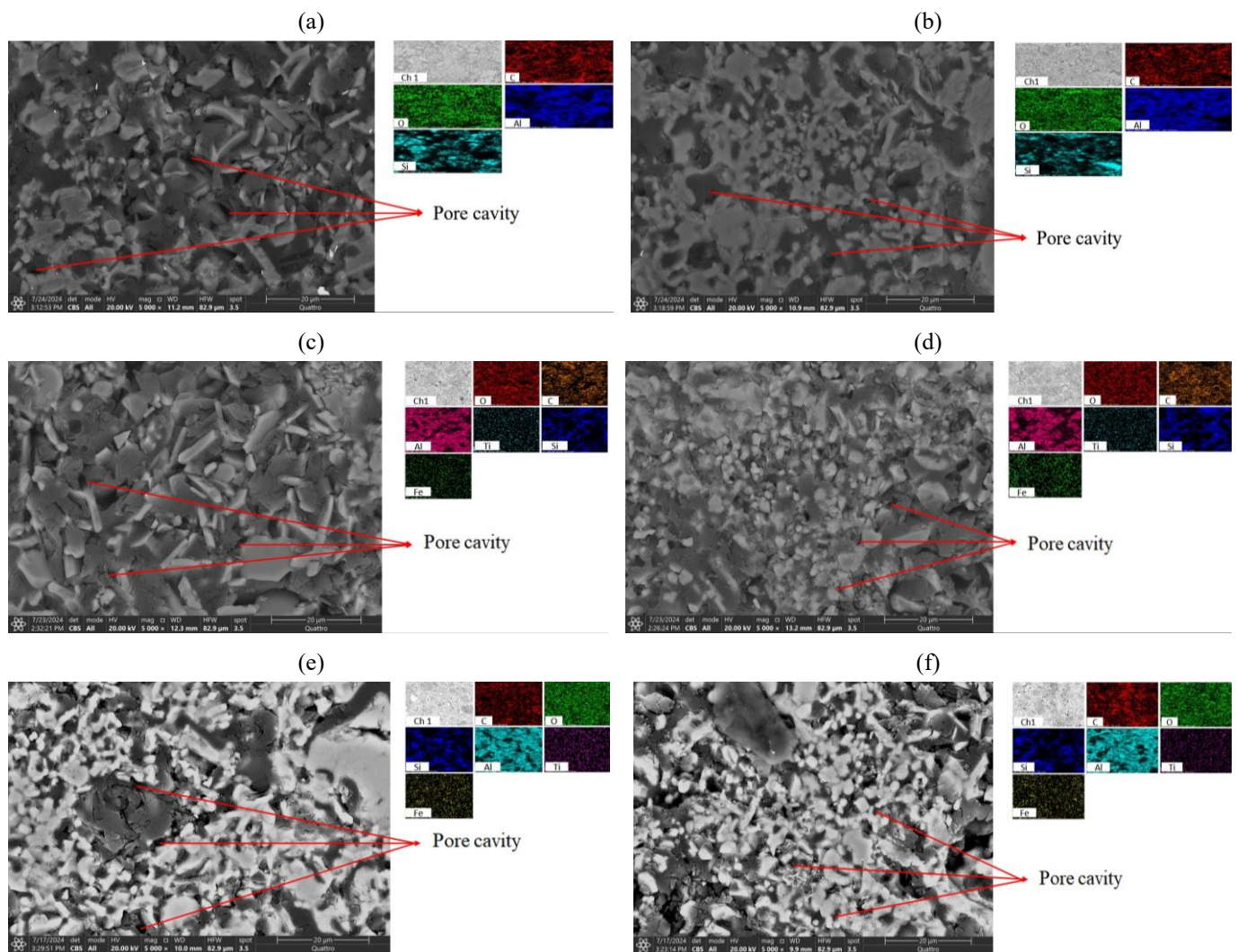


Figure 3. SEM micrographs of the refractory samples: (a) RF20/30/50A; (b) RF20/30/50B; (c) RF15/35/50A; (d) RF15/35/50B; (e) RF10/40/50A; f – RF10/40/50B

In conclusion, the presence of pore cavities within refractory bricks is a significant factor that affects their overall performance. Effective control of heating conditions is crucial for minimizing the formation of these voids, thereby enhancing the material's mechanical strength, thermal properties, and durability.

In the density analysis shown in Figure 4a, the variation RF 15/35/50A is found to have the highest density value of 2.13 g/cm<sup>3</sup>. This observation is supported by the SEM analysis in Figure 3c, which shows that the topography of variation RF15/35/50A exhibits the highest density, characterized by smaller and fewer pore cavities. The density of the refractory brick samples is influenced by the heating temperature, with samples treated at 1300°C showing a density increase of approximately 2-3 g/cm<sup>3</sup> compared to those treated at 1200°C. This increase in mass density is consistent with previous research, which indicates that mass density tends to rise with increasing temperature [20].

The improvement in the density of sample variations can be attributed to the reaction of silica oxide, which acts as a nucleating agent that triggers diffusion reactions at higher temperatures. This results in increased density and reduced pore cavities [26]. The diffusion of grains and the reaction of the nucleating agent help eliminate pores between grains, thereby reducing porosity and increasing bulk density as the temperature rises [27].

Conversely, the porosity values are inversely proportional to the density values. As shown in Figure 4b, the porosity of each sample is relatively high, surpassing the standard porosity limit for high alumina fire bricks (HA-50) set by ASTM C134-95 with values ranging from 20 to 24% [28]. This is consistent with the SEM analysis in Figure 3, which shows visible empty gaps or pore cavities in the topography of the refractory brick samples. The high porosity could be due to insufficient pressure applied during the molding process of the refractory brick samples, which were subjected to a 10-ton pressure treatment. Chen et al applied a 20-ton pressure treatment during the sample molding process, which had a notable impact on the physical properties of the bricks [29]. Similarly, Wembe et al used a 16-ton pressure treatment, also demonstrating a significant effect on the physical properties of refractory bricks [30].

Regarding the water absorption analysis in Figure 4c, the variation samples 20/30/50 and 10/40/50 exhibit the highest water absorption percentage at 16%. These values exceed the limit for high alumina refractory bricks, as defined by ASTM C134-95, which sets the maximum water absorption value at 5% [28]. This higher water absorption is directly linked to the high porosity and pore cavities in the refractory bricks, as confirmed by both the porosity and SEM analyses. The increase in water absorption capacity correlates with the increase in porosity and the presence of pore cavities in the bricks [31].

The results of the permanent linear change analysis, presented in Figure 5a, indicate that the highest shrinkage values are observed in samples RF20/30/50A and RF15/35/50A, both of which show a shrinkage of 8%. This shrinkage in volume is attributed to the heating rate reaction, which leads to adjustments in the compaction of the mass structure of these variations [32]. These findings align with the STA analysis results, which indicate that at temperatures between 100 and 200°C, the material undergoes decomposition due to the release of compounds.

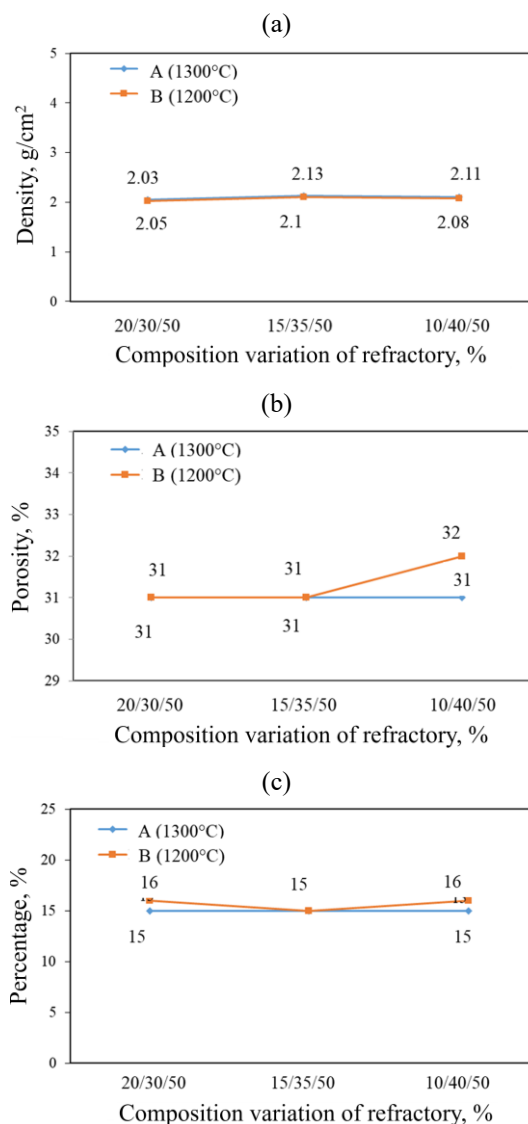


**Figure 4. Results test of composition variation refractory: (a) density; (b) porosity; (c) water absorption analysis**

In contrast, at temperatures ranging from 1000 to 1300°C, oxidation of alumina and silica compounds occurs, resulting in the formation of the mullite phase. Coppola et al confirmed that shrinkage is linked to dehydration and hydroxylation processes occurring between 200 and 500°C. In comparison, at temperatures between 800 and 1000°C, shrinkage is primarily associated with softening, viscous sintering, and structural rearrangement [33].

The observations indicated that samples RF20/30/50A through RF10/40/50A, which were heated to 1300°C, exhibited higher shrinkage percentages than those treated at 1200°C. This difference is attributed to the varying heating temperatures, which directly influence the shrinkage. As the temperature increases, low-melting oxides in clay minerals are more likely to contribute to the melting of products within the structure, thereby increasing the shrinkage value [34].

Regarding the cold crushing strength (CCS) analysis in Figure 5b, RF15/35/50A demonstrated the highest strength value of 26.54 MPa. This superior strength can be attributed to the high mass density and relatively small number of pore cavities in the structure of RF15/35/50A. These findings are supported by the SEM analysis shown in Figure 3c and the density analysis results in Figure 4a.

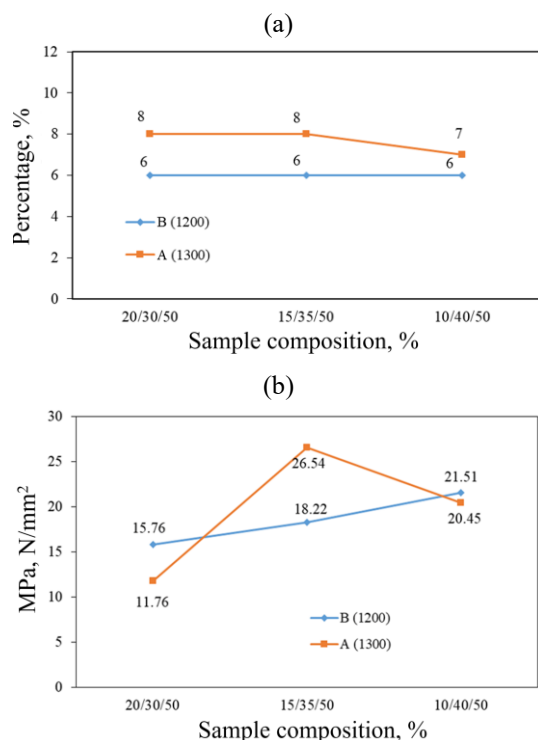


Figure 5. Results of physical property analysis: (a) PLC; (b) CCS

Comparison of the variation samples treated at 1300°C revealed varying CCS values, which can be explained by the different reactions occurring during the heating process, as evidenced by the STA analysis in Figure 2.

In contrast, sample variations RF20/30/50B through RF10/40/50B, which were treated at 1200°C, displayed an increasing trend in CCS values. This increase can be attributed to the differences in component composition, as higher silica (SiO<sub>2</sub>) content tends to lower the compressive strength of the material [34]. This observation is consistent with the CCS values obtained for samples heated at 1200°C, as confirmed by the XRF analysis presented in Table 2.

The chemical property analysis of the refractory bricks, as shown in Figure 6, reveals that the variation samples exposed to a sulfuric acid (H<sub>2</sub>SO<sub>4</sub>) solution did not exhibit any corrosive reaction after being reheated at 1150°C. This behavior can be attributed to the composition of the refractory brick sample, as indicated by the XRF analysis results in Table 2, which show a dominant presence of SiO<sub>2</sub>. Silica oxide is known for its high resistance to acidic environments, effectively inhibiting the penetration of corrosive acid properties. In contrast, the variation samples treated with a sodium hydroxide (NaOH) solution showed signs of blackening after reheating [35]. This blackened area is likely a result of the corrosive penetration effect of the alkaline solution interacting with the silica oxide component. Silica is highly reactive and tends to form bonds or react with other compounds [10].



Figure 6. Chemical resistance test: (a) with H<sub>2</sub>SO<sub>4</sub>; (b) with NaOH

This observation aligns with the findings of Barandehfard et al. and Weinberg et al., who investigated the degradation mechanisms of corrosion properties [6], [36]. They noted that after the penetration of corrosive agents, a side wall accumulation or volume expansion may occur, which negatively affects the material's resistance capabilities and shortens its service life. This phenomenon is consistent with the results observed in the NaOH-exposed samples, where volume expansion occurred due to the alkaline solution, which left behind sediment residues from the heating reaction.

Based on the findings and limitations identified in this study, future research will focus on optimizing the forming pressure and exploring advanced sintering profiles to further enhance the microstructural and mechanical properties of the refractory bricks. The primary objectives are to:

1) systematically investigate the impact of higher forming pressures (e.g., 15-25 tons) on reducing porosity and improving density to meet the ASTM standard for high-alumina bricks;

2) develop and apply a multi-stage sintering profile with specific holding phases to better control mullite crystallization and grain growth, aiming to minimize residual pore cavities.

The significance of this proposed study lies in bridging the gap between the promising composition developed here and industrial-grade performance standards. By addressing the key processing parameters of pressure and thermal cycle, this future research aims to translate the sustainable, cost-effective material formulation into a viable, high-performance refractory product with consistently superior mechanical strength, thermal shock resistance, and lower permeability for demanding industrial applications.

#### 4. Conclusions

The detailed analytical investigation of alumina-based refractory bricks clearly demonstrates that the interplay between raw material composition and firing treatment parameters critically determines their physical properties, microstructural development, and functional performance. Among the various formulations studied, sample RF15/35/50A, when subjected to a precisely controlled firing regime at 1300°C, exhibited the highest cold crushing strength (CCS) of 26.54 N/mm<sup>2</sup>. This elevated mechanical strength is indicative of an optimized sintering process, resulting in enhanced densification and robust interparticle bonding that minimizes defects, such as microcracks and porosity, thereby improving the material's load-bearing capacity under compressive stresses.

Complementing these mechanical properties, density analysis identified sample variation two as having the highest interparticle density of 2.13 g/cm<sup>3</sup>, suggesting a significantly reduced porosity and a compact microstructure. This densification is critical in enhancing resistance to thermal shock, mechanical wear, and chemical ingress, ensuring prolonged structural integrity in demanding environments. Chemical resistance assessments further revealed that this sample exhibits superior resistance to acid abrasion, a vital characteristic for refractory materials exposed to harsh acidic conditions in industrial processes such as chemical reactors and incinerators.

High-resolution Field Emission Scanning Electron Microscopy (FE-SEM) characterization provided deep insights into the microstructural features of sample RF15/35/50A, revealing tightly bonded grains with minimal intergranular voids, which correlate strongly with the observed high mechanical strength. Moreover, the FE-SEM images confirmed the presence of a

well-developed mullite ( $3\text{Al}_2\text{O}_3 \cdot 2\text{SiO}_2$ ) phase, formed through solid-state reactions among aluminum, silicon, and oxygen atoms during the firing process. The homogeneous and uniform distribution of mullite crystals within the matrix is pivotal, as mullite's intrinsic properties, such as high melting point ( $\sim 1840^\circ\text{C}$ ), low thermal expansion coefficient, and exceptional thermal and chemical stability, contribute significantly to enhancing the refractory's resistance to thermal degradation, mechanical stresses, and chemical corrosion. This mullite network acts to reinforce the ceramic matrix by limiting grain boundary sliding and crack propagation, thereby improving thermal shock resistance and durability.

Collectively, these findings underscore that the careful optimization of alumina content, supplementary raw materials, and firing temperature orchestrates the formation of a dense, mullite-reinforced microstructure, which in turn delivers enhanced mechanical strength, chemical durability, and thermal stability. Such tailored refractory bricks are therefore well-suited for high-temperature industrial applications where materials must withstand aggressive mechanical, thermal, and chemical conditions over prolonged service periods, underscoring the critical role of precise compositional and processing control in the development of advanced refractory materials.

#### Author contributions

Conceptualization: DCB, AM; Data curation: MA, SUD; Formal analysis: DCB, FHJ, AM; Funding acquisition: FHJ, SUD; Investigation: DCB, MA; Methodology: DCB, FHJ, MKN, DMP; Project administration: DCB, AM, DMP; Resources: MA, FHJ, SUD; Software: AM, MKN, DMP; Supervision: DCB, AM; Validation: DCB, MA; Visualization: AM, FHJ, SUD; Writing – original draft: DCB, MKN, DMP; Writing – review & editing: MA, AM, FHJ, SUD. All authors have read and agreed to the published version of the manuscript.

#### Funding

This research was funded by the Research Organization for Nanotechnology and Materials, BRIN, through the Rumah program funding research. All sources of funding for the study should be disclosed.

#### Acknowledgements

The authors acknowledge the facilities and scientific and technical support from the Minerals Laboratory Lampung, National Research and Innovation Agency, through E-Layanan Sains, Badan Riset dan Inovasi Nasional (BRIN).

#### Conflicts of interest

The authors declare no conflict of interest.

#### Data availability statement

The original contributions presented in the study are included in the article, further inquiries can be directed to the corresponding author.

#### References

- [1] Yin, B., Li, Y., Wang, S., & Zheng, Y. (2023). Corrosion resistance of calcium hexaaluminate insulating firebrick for synthesising ternary lithium-ion battery cathode materials. *Journal of Alloys and Compounds*, 942, 168953. <https://doi.org/10.1016/j.jallcom.2023.168953>
- [2] ASTM C71-12. (2018). *Standard terminology relating to refractories*. West Conshohocken, United States: ASTM International.
- [3] Mouiya, M., Tessier-Doyen, N., Tamraoui, Y., Alami, J., & Huger, M. (2023). High temperature thermomechanical properties of a microcracked model refractory material: A silica-doped aluminium titanate. *Ceramics International*, 49(14), 24572-24580. <https://doi.org/10.1016/j.ceramint.2023.01.027>
- [4] Anwar, A., Rhozman, F., & Nadliroh, K. (2020). Pengaruh perbedaan ketebalan semen alumina 4 cm dan 5 cm terhadap kemampuan menahan panas. *Seminar Nasional Inovasi Dan Teknologi*, 190-195.
- [5] Gu, F., Zhang, Y., Tu, Y., Wu, X., Zhu, Y., Long, Y., & Shen, D. (2022). Assessing magnesia effect on preparing refractory materials from ferrochromium slag. *Ceramics International*, 48(9), 13100-13107. <https://doi.org/10.1016/j.ceramint.2022.01.186>
- [6] Barandehfard, F., Aluha, J., Hekmat-Ardakan, A., & Gitzhofer, F. (2020). Improving corrosion resistance of aluminosilicate refractories towards molten Al-Mg alloy using non-wetting additives: A short review. *Materials*, 13(18), 4078. <https://doi.org/10.3390/ma13184078>
- [7] Syukuriah, S., Hustim, M., Tjaronge, W., & Irmawaty, R. (2025). Performance evaluation of magnesia-type refractory brick waste as complete replacement for fine aggregate and filler in asphalt concrete wearing course mixtures. *Engineering, Technology & Applied Science Research*, 15(1), 19575-19582. <https://doi.org/https://doi.org/10.48084/etasr.9298>
- [8] Kuntaarsa, A. (2017). Perbaikan mutu bodi keramik lempung Pundong dengan penambahan pecahan kaca lampu neon bekas. *Eksergi*, 14(2), 62-71. <https://doi.org/10.31315/e.v14i2.2149>
- [9] Daud, D. (2015). Kaolin sebagai bahan pengisi pada pembuatan komposit karet: Pengaruh ukuran dan jumlah terhadap sifat mekanik-fisik. *Jurnal Dinamika Penelitian Industri*, 26(1), 41-48.
- [10] Handoko, D., & Pujarianto, P. (2024). Pengaruh komposisi pasir kuarsa terhadap sifat bata tahan api (firebrick) berbahan kaolin dan fly ash. *Jurnal Mesin Nusantara*, 7(1), 113-125. <https://doi.org/10.29407/jmn.v7i1.21978>
- [11] El Haddar, A., Manni, A., Azdimousa, A., El Hassani, I.E.E.A., Bellil, A., Sadik, C., & El Ouahabi, M. (2020). Elaboration of a high mechanical performance refractory from halloysite and recycled alumina. *Boletín de la Sociedad Española de Cerámica y Vidrio*, 59(3), 95-104. <https://doi.org/10.1016/j.bsecv.2019.08.002>
- [12] Amin, M., Suryana, Y.I., Isnugroho, K., Aji, B.B., Birawidha, D.C., & Hendronursito, Y. (2018). Characterization of refractory brick based on local raw material from Lampung Province – Indonesia. *AIP Conference Proceedings*, 1945(1), 020047. <https://doi.org/10.1063/1.5030269>
- [13] ASTM C113-14. (2019). *Standard test method for reheat change of refractory brick*. West Conshohocken, United States: ASTM International.
- [14] Sawadogo, M., Seynou, M., Zerbo, L., Sorgho, B., Laure Lecomte-Nana, G., Blanchart, P., & Ouédraogo, R. (2020). Formulation of clay refractory bricks: influence of the nature of chamotte and the alumina content in the clay. *Advances in Materials*, 9(4), 59-67. <https://doi.org/10.11648/j.am.20200904.11>
- [15] Chargui, F., Hamidouche, M., Belhouchet, H., Jorand, Y., Doufounou, R., & Fantozzi, G. (2018). Mullite fabrication from natural kaolin and aluminium slag. *Boletín de La Sociedad Española de Cerámica y Vidrio*, 57(4), 169-177. <https://doi.org/10.1016/j.bsecv.2018.01.001>
- [16] Liu, Z., Lian, W., Liu, Y., Zhu, J., Xue, C., Yang, Z., & Lin, X. (2021). Phase formation, microstructure development, and mechanical properties of kaolin-based mullite ceramics added with  $\text{Fe}_2\text{O}_3$ . *International Journal of Applied Ceramic Technology*, 18(3), 1074-1081. <https://doi.org/10.1111/ijac.13720>
- [17] Luz, A.P., Gagliarde, J.H., Aneziris, C.G., & Pandolfelli, V.C. (2017). B4C mineralizing role for mullite generation in  $\text{Al}_2\text{O}_3$ - $\text{SiO}_2$  refractory castables. *Ceramics International*, 43(15), 12167-12178. <https://doi.org/https://doi.org/10.1016/j.ceramint.2017.06.075>
- [18] Kotrbová, L., Uhlířová, T., Pabst, W., Hubálková, J., & Kotouček, M. (2025). Thermal conductivity of silica refractories and its temperature dependence during thermal cycling, compared to silicite and sandstone. *Open Ceramics*, 21, 100735. <https://doi.org/10.1016/j.oceram.2025.100735>
- [19] Reverdatto, V.V., Likhanov, I.I., Polyansky, O.P., Sheplev, V.S., & Kolobov, V.Y. (2019). *The nature and models of metamorphism*. Springer International Publishing.
- [20] Bella, M.L., Hamidouche, M., & Gremillard, L. (2021). Preparation of mullite-alumina composite by reaction sintering between Algerian kaolin and amorphous aluminum hydroxide. *Ceramics International*, 47(11), 16208-16220. <https://doi.org/10.1016/j.ceramint.2021.02.199>
- [21] Wesolowski, M., & Leyk, E. (2023). Coupled and simultaneous thermal analysis techniques in the study of pharmaceuticals. *Pharmaceutics*, 15(6), 1596. <https://doi.org/https://doi.org/10.3390/pharmaceutics15061596>
- [22] Yue, X., Li, Y., Li, H., Ma, C., & Zhang, X. (2022). Phase evolution of a novel silicon-alumina-fused mullite-containing  $\text{Ti}_2\text{O}_3$  refractory at  $1300^\circ\text{C}$  in  $\text{N}_2$ . *Ceramics International*, 48(21), 31686-31694. <https://doi.org/10.1016/j.ceramint.2022.07.090>

- [23] Guo, D., Li, X., Chen, P., Zhu, B., & Fang, B. (2016). Microstructure evolution and its effect on thermo-mechanical properties of low-carbon Al<sub>2</sub>O<sub>3</sub>-C refractories. *Ceramics International*, 42(16), 19071-19078. <https://doi.org/https://doi.org/10.1016/j.ceramint.2016.09.066>
- [24] Peng, Z., Sun, W., Xiong, X., Zhang, H., Guo, F., & Li, J. (2021). Novel refractory high-entropy ceramics: Transition metal carbonitrides with superior ablation resistance. *Corrosion Science*, 184, 109359. <https://doi.org/10.1016/j.corsci.2021.109359>
- [25] Weidner, A., Ranglack-Klemm, Y., Zienert, T., Aneziris, C.G., & Biermann, H. (2019). Mechanical high-temperature properties and damage behavior of coarse-grained alumina refractory metal composites. *Materials*, 12(23), 3927. <https://doi.org/10.3390/ma12233927>
- [26] Díaz-Tato, L., Lopez-Perales, J.F., Contreras, J.E., Banda-Muñoz, F., Suárez-Suárez, D., González-Carranza, Y., & Rodríguez, E.A. (2022). Hydration resistance and mechano-physical properties improvement of a magnesia-dolomite dense refractory by hercynite spinel. *Materials Chemistry and Physics*, 287, 126314. <https://doi.org/10.1016/j.matchemphys.2022.126314>
- [27] Michel, R., Ammar, M.R., Poirier, J., & Simon, P. (2013). Phase transformation characterization of olivine subjected to high temperature in air. *Ceramics International*, 39(5), 5287-5294. <https://doi.org/https://doi.org/10.1016/j.ceramint.2012.12.031>
- [28] ASTM C134-95. (2023). *Standard test methods for size, dimensional measurements, and bulk density of refractory brick and insulating firebrick*. West Conshohocken, United States: ASTM International.
- [29] Chen, Z., Yan, W., Schafföner, S., Zhi, J., & Li, N. (2022). High-strength microporous corundum-mullite refractory aggregates with sub-micron pores using vacuum impregnation treatment. *Journal of Materials Research and Technology*, 19, 3433-3442. <https://doi.org/10.1016/j.jmrt.2022.06.091>
- [30] Tiegoum Wembe, J., Mambou Ngueyep, L.L., Tchognia Nkuissi, H.J., Tchedeleg Langollo, Y., Tchioffo Tiwa, I.C., Pliya, P., & Ndjaka, J.M.B. (2024). Mineralogical, chemical and physico-mechanical properties of fired bricks for refractory industry applications. *Discover Soil*, 1(1), 5. <https://doi.org/10.1007/s44378-024-00005-4>
- [31] Samad, A., Baidya, S., Akhtar, U.S., Ahmed, K.S., Roy, S.C., & Islam, S. (2021). Manufacture of refractory brick from locally available red clay blended with white Portland cement and its performance evaluation. *GEOMATE Journal*, 20(80), 105-112. <https://doi.org/https://doi.org/10.21660/2021.80.j2033>
- [32] Huang, L., Pan, Y., Zhang, J., Du, Y., Zhang, Y., & Zhang, S. (2021). Densification, grain growth mechanism and mechanical properties of Mo10Nb refractory targets fabricated by SPS. *International Journal of Refractory Metals and Hard Materials*, 99, 105575. <https://doi.org/10.1016/j.ijrmhm.2021.105575>
- [33] Coppola, B., Tardivat, C., Richaud, S., Tulliani, J. M., Montanaro, L., & Palmero, P. (2020). Alkali-activated refractory wastes exposed to high temperatures: development and characterization. *Journal of the European Ceramic Society*, 40(8), 3314-3326. <https://doi.org/10.1016/j.jeurceramsoc.2020.02.052>
- [34] Hossain, S.S., & Roy, P.K. (2019). Fabrication of sustainable insulation refractory: Utilization of different wastes. *Boletín de la Sociedad Española de Cerámica y Vidrio*, 58(3), 115-125. <https://doi.org/10.1016/j.bsecv.2018.09.002>
- [35] Valenzuela-Gutierrez, A., Lopez-Cuevas, J., Gonzalez-Angeles, A., & Pilalua-Diaz, N. (2019). Addition of ceramics materials to improve the corrosion resistance of alumina refractories. *SN Applied Sciences*, 1(7), 784. <https://doi.org/10.1007/s42452-019-0789-5>
- [36] Weinberg, A.V., Varona, C., Chaucherie, X., Goeuriot, D., & Poirier, J. (2017). Corrosion of Al<sub>2</sub>O<sub>3</sub>-SiO<sub>2</sub> refractories by sodium and sulfur vapors: A case study on hazardous waste incinerators. *Ceramics International*, 43(7), 5743-5750. <https://doi.org/https://doi.org/10.1016/j.ceramint.2017.01.116>

## Вплив складу алюмооксидних матеріалів та температури випалу вогнетривкої цегли на формування муліту

Д.Ч. Біравідха, М. Амін, А. Місванто, Ф.Х. Джая, С.У. Деві, М.К. Нарісварі, Д.М. Путрі

**Мета.** У роботі досліджено вплив вмісту оксиду алюмінію та температури випалу на процес формування муліту у вогнетривких цеглах, виготовлених на основі каоліну, глинозему та вторинного шамоту. Метою дослідження є створення високоєфективних і економічно доцільних вогнетривких матеріалів із використанням місцевої та переробленої сировини.

**Методика.** Для виконання дослідження було підготовлено три склади з різним вмістом глинозему, які формували методом пресування та спікали при температурах 1200 і 1300°C. Хімічний склад визначали методом рентгенофлуоресцентного аналізу (XRF), фазовий склад – рентгенофазовим аналізом (XRD), мікроструктуру – за допомогою FE-SEM/EDX, а термічну поведінку – методами синхронного термічного аналізу (STA). Механічні властивості визначали із використанням універсальної випробувальної машини (UTM), а хімічну стійкість оцінювали шляхом витримування зразків у розчинах H<sub>2</sub>SO<sub>4</sub> та NaOH.

**Результати.** Встановлено, що підвищення вмісту глинозему та випал при температурі 1300°C сприяють інтенсифікації формування муліту, що зумовлює зростання механічної міцності, об'ємної щільності, а також стійкості до термічних ударів і хімічної корозії. Найкращі показники продемонстрував вогнетривкий матеріал із вмістом 35% глинозему, випалений при 1300°C, для якого досягнуто максимальну межу міцності при стиску (26.5 Н/мм<sup>2</sup>) та об'ємну щільність 2.13 г/см<sup>3</sup>, що свідчить про оптимальні експлуатаційні характеристики.

**Наукова новизна.** Новизна дослідження полягає у цілеспрямованому використанні вторинного шамоту не лише як інертного наповнювача, а як функціонального попередника муліту, що взаємодіє з місцевим каоліном і підвищує ефективність спікання. Це підтверджено високими механічними та фізичними показниками складу з 35% глинозему, випаленого при 1300°C, що вказує на можливість отримання високоякісних вогнетривків з екологічно сталих джерел сировини.

**Практична значимість.** Отримані результати створюють практичні передумови для виробництва якісних вогнетривких матеріалів із використанням місцевої та переробленої сировини, зменшуючи залежність від чистого глинозему та сприяючи екологічній сталості виробництва.

**Ключові слова:** вогнетривка цегла, муліт, випробування, аналіз, глинозем

## Publisher's note

All claims expressed in this manuscript are solely those of the authors and do not necessarily represent those of their affiliated organizations, or those of the publisher, the editors and the reviewers.